

Thermal Damage Evaluation of a Limestone Using Ultrasonic Velocity and Resonant Frequency

C. Kazemi, C. V. Cedeño-Burgos, V. Martínez-Ibáñez & M. E. Garrido
*Universitat Politècnica de València, València, Spain
ckazemi@doctor.upv.es*

Á. Rabat
Universidad de Alicante, Alicante, Spain

Abstract

In some cases, such as fires in monuments or historical infrastructures, rocks are subjected to extreme temperatures, affecting their physical and mechanical properties. The present study uses two non-destructive techniques, the resonant frequency, and ultrasonic pulse velocity tests, to evaluate thermal damage in a limestone exposed to different temperatures. To complete and contrast the results of these tests, Scanning Electron Microscopy images were obtained. The heat treatment in this research involved exposing the sample to different target temperatures, 200, 400, and 600°C, followed by cooling by immersion in water. The resonant frequency and ultrasonic pulse velocity test results were compared before and after the heat exposure. As a result of heat exposure, the ultrasonic pulse velocity and the resonant frequency decreased as target temperatures increased, and the latest shows a considerable discrepancy. These discrepant fluctuations included the increased extension of the wave period when compared to its altitude in all three types of waves: longitudinal, transversal, and torsional. Furthermore, the decrease in wave frequency was evident as the target temperature increased. These results reveal the appearance of micro-cracks within the rock mass. Microscopy images were performed on the specimens to approve this assumption. The rising number of micro-cracks by the target temperature increment as an output of microscopy clarifies the effects on wave propagation velocity.

Keywords

Ultrasonic pulse velocity, resonant frequency, limestone, heat exposure, SEM



1. Introduction

Limestone, a widely used sedimentary rock, is valued for its aesthetic and structural properties. However, exposure to elevated temperatures, as occurs in fire scenarios or industrial processes, can lead to thermal damage, altering its physical and mechanical properties. Evaluating the extent of such damage is essential for assessing the rock's residual strength and durability.

Research has demonstrated that elevated temperatures can lead to substantial changes in the mechanical properties of limestone which in some cases may reach up to 160 MPa in uniaxial compressive strength (Hassanpour et al., 2024), and a wide range in tensile strength (Kazemi and Cheshomi, 2022). Tufail et al. (2017) investigated the effects of high temperatures on various types of rocks, including limestone. They found that thermal exposure can cause a reduction in compressive strength, an increase in porosity, and a significant decrease in ultrasonic wave velocity (Martínez-Ibañez et al., 2021a), which directly correlates with the mechanical performance of concrete structures involving limestone aggregates. Similarly, González-Gómez et al. (2015) examined thermal effects on the physical properties of limestones and concluded that exposure to heat alters density and elasticity, resulting in increased brittleness. Martínez-Ibañez et al. (2021) assessed the effects of high temperature on a sample from a limestone formation in Spain as a feasibility study for a tunnel construction project prone to fire incidents. The study indicated that the elevation of temperature not only alters the structure of limestones but also changes the chemical composition. Liu et al. (2024) tested limestone heat-treated rocks mechanically and figured out that all compressive properties and tensile properties of these rocks were affected. Eljufout et al. (2021) established an in-situ model for evaluating the mechanical properties of rocks by ultrasonic pulse velocity, which is a non-destructive test. Garrido et al. (2023) acquired a considerable drop in the results of the point load test on limestone specimens as an effect of heat exposure. Feng et al. (2021) research shows that heat exposure significantly drops the stress required for crack initiation in limestones.

This study employs ultrasonic pulse velocity (hereafter UPV) and resonant frequency (hereafter RF) tests, two non-destructive techniques widely used to evaluate the integrity of rock materials. This research aims to elucidate the thermal damage in limestone by analyzing changes in UPV and RF after heat exposure.

2. Materials and Methods

2.1. Materials and samples preparation

The samples used in this study are limestones obtained from a quarry of Elda (Alicante, Eastern Spain). The limestone is characterized by a fine-grained texture and homogeneity, typical of sedimentary carbonate rocks. This rock is known as “Blue Bateig” limestone and has been widely used in construction for centuries. The quarry provided prismatic blocks with dimensions of 300×140×100 mm. From these blocks, cylindrical samples were extracted. These samples were divided into groups and subjected to specific target temperatures: 200, 400, and 600°C.

The samples were prepared according to standard dimensions (Aydin, 2014; ASTM, 2008) for ultrasonic pulse velocity and resonant frequency tests, each containing five cylindrical specimens to undergo heat exposure at the mentioned target temperatures. After cutting and polishing, the sample dimensions were a diameter of 54.8 ± 0.4 mm and a height of 153.0 ± 1.7 mm, and the slenderness was slightly greater than 2.5. This study employs ultrasonic pulse velocity (hereafter UPV) and resonant frequency (hereafter RF) tests, two non-destructive techniques widely used to evaluate the integrity of rock materials. This research aims to elucidate the thermal damage in limestone by analyzing changes in UPV and RF after heat exposure.

2.2. Testing Procedures

Assessing the thermal damage in specimens of the present study requires a comparison between the results of the tests before and after the heating phase, which herein are called the prior and posterior tests, respectively. The temperature at which the tests are performed could affect the results. Hence, the

temperature of each specimen was recorded by an infrared thermometer. In Fig 1 Workflow of the research, a general scheme of this study's procedure is depicted.

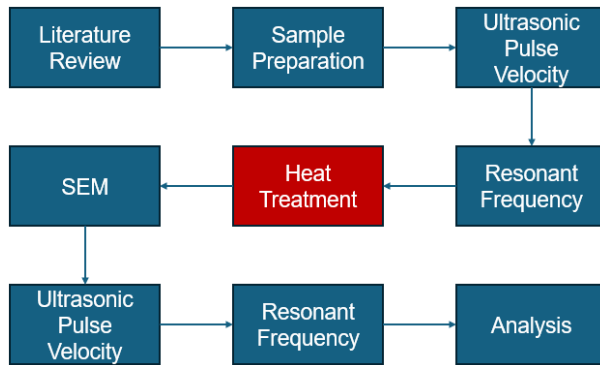


Fig 1 Workflow of the research

2.2.1. SEM Microscopy

The samples were analyzed using the Scanning Electron Microscope (SEM) shown in Fig. 2. This technique provided high-resolution and high-magnification images. The equipment used was a Field Emission Scanning Electron Microscope (FESEM), model ZEISS ULTRA 55, belonging to the microscopy service of the Universitat Politècnica de València.



Fig. 2 SEM Microscopy setup

2.2.2. Ultrasonic Pulse Velocity Test

UPV tests were conducted on the specimens, as shown in Fig. 3a, according to the ISRM standard (Aydin, 2014). Before starting the tests, the device was calibrated utilizing a calibration cylinder. Then, the specimens were kept firmly between the transducers by a grip. To mitigate the errors of measuring the transit time of ultrasonic waves through the rock due to the possibility of mild curvatures in ending surfaces of the specimens, a thin lamina of a special gel was used to cover and balance such meager irregularities. At last, the UPV was calculated using the equation proposed by the standard.

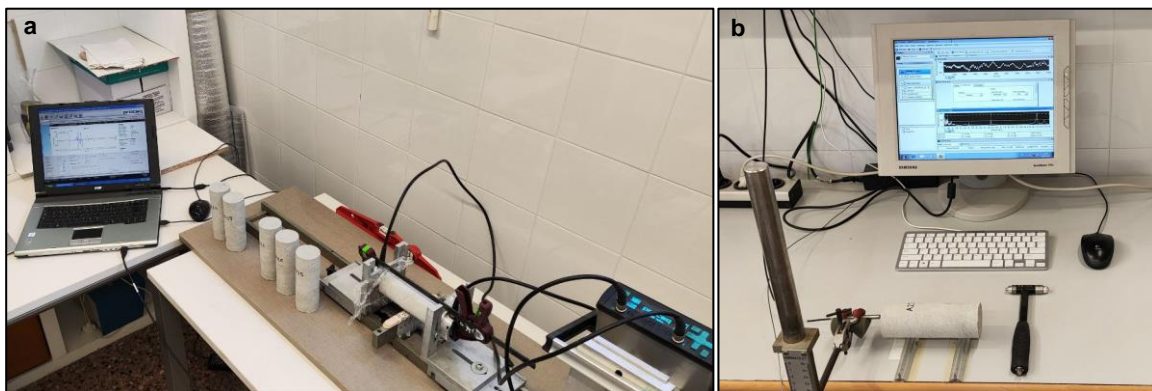


Fig. 3 Equipment setups used for: a) Ultrasonic Pulse Velocity, b) Resonant Frequency

2.2.3. Resonant Frequency Test

The RF test involved the measurement of the natural frequency of vibration of the specimens using a resonant frequency analyzer, which is indicated in Fig. 3b. The transverse, longitudinal, and torsional frequencies were recorded according to ASTM C215 (2008) to assess the effects of heat exposure on

the microstructural phenomenon and the material's overall integrity. For this, specimens were held steady above the shelf by two slender holders. This way of preserving the specimens minimized the absorption of dynamic energy produced by the hammer. Specimens were hit by the hammer in three different positions to obtain three peaks of the aforementioned frequency types throughout the spectrum. During all readings and test processes within this research, the temperature of specimens was 25.5°C, measured by an infrared thermometer before starting the tests.

2.2.4. Heat Treatment

Once the specimens were finished with the primary measurements of UPV and RF, they were subjected to heat treatment in a muffle furnace up to 200, 400, and 600°C, as the most common temperature values within previous studies in rock mechanics (Altuğ and Soeylemez, 2023). The heating rate was 5°C/min, and the temperature was maintained for 1 hour at the target value, after which the specimens were quenched in 70°C water and later dried in an oven at 70°C.

3. Results

3.1. Ultrasonic Pulse Velocity

The UPV results showed a progressive decline both for S-waves and P-waves with increasing temperature, illustrated in Fig. 4a and Fig. 4b, respectively. The average value of P-wave and S-wave velocities for all the specimens in the unheated state are approximately 3722 and 2119 m/s, respectively. The average reduction in P-wave velocity for specimens from 200, 400, and 600°C ranges from 1.5% to 18.6% and 40.6%, respectively. The average decrease of S-wave velocity for 200, 400, and 600°C specimens are 2.9%, 14.7%, and 34.1%, respectively. The P-waves face a greater reduction for 400 and 600°C specimens than S-waves.

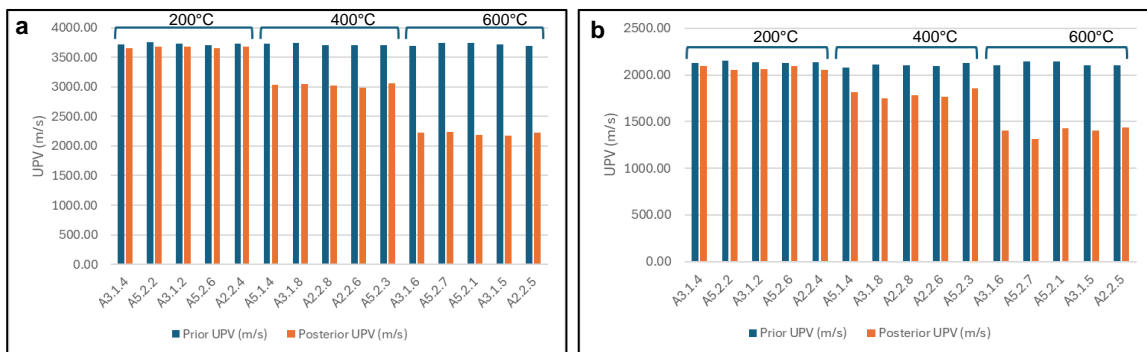


Fig. 4 UPV results prior to heat exposure (Blue) and posterior to heat exposure (Orange) for: a) P-wave, and b) S-wave

3.2. Resonant Frequency

The average values for the total statistical society of specimens before the heating stage are 5816 Hz, 11466 Hz, and 12440 Hz for transversal, longitudinal, and torsional RFs, respectively. The RF results similarly demonstrated significant decreases in transversal, longitudinal, and torsional frequencies with increasing temperatures, as shown in Fig. 5 for the average results after heat exposure.

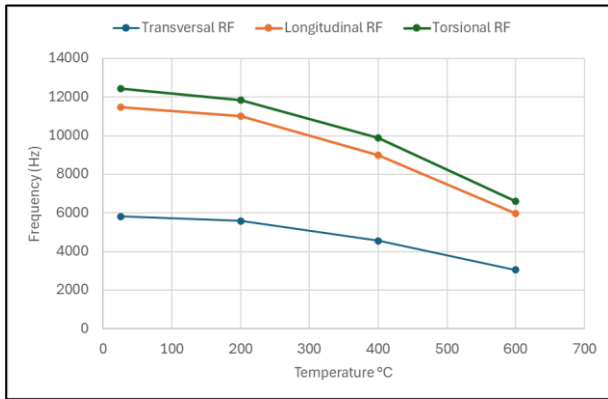


Fig. 5 Average RFs variations in different groups of temperature

The average decrease in Transversal RF for the thermal groups at 200, 400, and 600°C is 3.6%, 21.7%, and 47.9%, respectively. For Longitudinal RF, the average reductions are 3.9%, 21.5%, and 47.9%, respectively. Similarly, the average reduction percentages for Torsional RF are 4.5%, 20.6%, and 47.1%, respectively. This reveals that the changes in Transversal RF, Longitudinal RF, and Torsional RF are pretty linear and relative to each other. In summary, all RF values are reduced by approximately a fifth of the total of 400°C, and they are reduced by almost half at 600°C.

4. Discussion

The study effectively highlights the impact of thermal damage on Blue Bateig limestone using non-destructive techniques: ultrasonic pulse velocity and resonant frequency tests.

4.1. Ultrasonic Pulse Velocity

The results indicate a progressive decline in UPV values as the temperature increases, especially at 600°C, where the reduction becomes severe. This trend aligns with the understanding that thermal stresses induce micro-cracking in the limestone, obstructing wave propagation.

- At 200°C, minor reductions in UPV (~3%) suggest initial micro-crack formation, possibly due to the expansion of mineral grains and water vaporization (Martínez-Ibáñez et al., 2021b).
- At 400°C, a steeper decline (~15%) occurs, indicating further propagation of cracks. This temperature range corresponds to thermal thresholds where certain minerals in limestone begin to alter structurally (Shen et al., 2018) or chemically (Martínez-Ibáñez et al., 2021b).
- At 600°C, the UPV reduction exceeds 30%, reflecting significant material degradation. This temperature likely promotes pore coalescence, inter-grain detachment, and thermal expansion beyond elastic limits (Yang et al., 2019).

These reductions demonstrate the compounding effect of thermal damage, as micro-cracks act as barriers, amplifying the wave attenuation.

The SEM microstructural analysis reinforces the mechanical findings by visualizing the micro-cracks and voids responsible for wave attenuation. The cracks are observed to increase in number and connectivity with temperature, transitioning from isolated fissures at 200°C to widespread networks at 600°C (Fig 6). These observations validate the hypothesis that thermal stress weakens the limestone through cumulative microstructural damage.

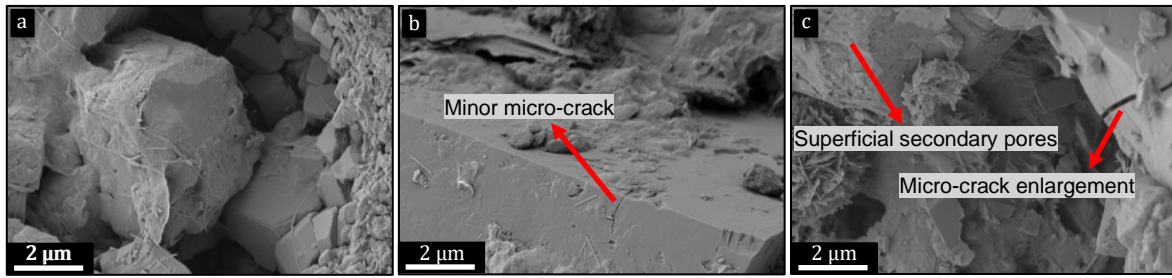


Fig 6 SEM microscopy images in 10k magnification: a) Sample lacks significant micro-cracks and secondary pores in 200°C, b) Sample with minor micro-cracks in 400°C, and c) Enlargement of micro-cracks and occurrence of superficial secondary pores in 600°C.

4.2. Resonant Frequency

The RF measurements complement the UPV findings, showing a marked decrease in all frequency types (transversal, longitudinal, and torsional) with rising target temperatures.

- The longitudinal RF reduced from 4% at 200°C to nearly 50% at 600°C. This drastic change highlights a significant loss of dynamic stiffness and rigidity, consistent with the thermal softening of minerals and crack proliferation.
- Similar trends were observed in transversal and torsional RF, though torsional waves appeared slightly less sensitive to thermal changes. The uniform degradation across frequencies suggests isotropic damage to the rock matrix.

The irregularities in RF data after heating further reflect heterogeneity in crack development, as seen in Fig. 6, where localized damage alters wave propagation paths and energy dissipation.

4.3. Comparative Analysis of UPV and RF

The study establishes a strong correlation between UPV and RF results, confirming the complementary nature of these techniques for evaluating thermal damage. While UPV directly measures wave speed as a proxy for rock density and elasticity, RF provides insight into the material's vibrational properties. Together, they offer a comprehensive view of the degradation process. The correlations between the changes of UPV (Δ UPV) and the changes of RF (Δ RF) results are indicated in Fig 7.

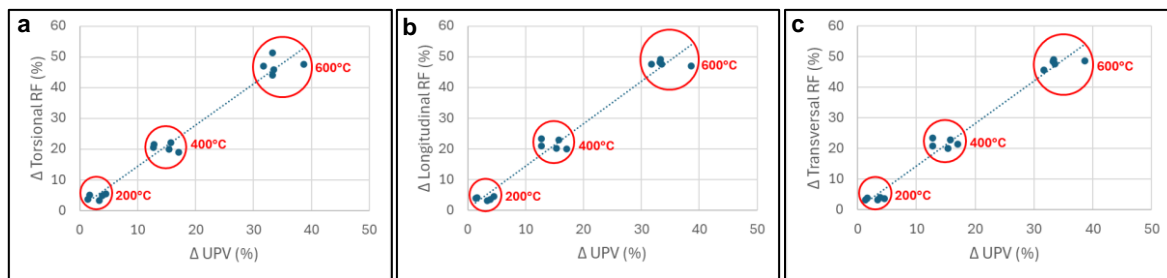


Fig 7 Correlation between Δ UPV and a) Δ Transversal RF, b) Δ Longitudinal RF, c) Δ Torsional RF

Each Δ RF factor demonstrates a strong linear relationship with Δ UPV by high coefficients of determination. Numerical amounts of Δ UPV and Δ RF are declines in percent according to the initial amount recorded before heat exposure. Suggested relationships are expressed in Table 1, along with coefficients of determination (R^2).

Table 1. Relationships between Δ RF and Δ UPV.

No.	Expression	R^2
1	Δ Transversal RF = 1.39 Δ UPV + 0.40	0.98
2	Δ Longitudinal RF = 1.38 Δ UPV + 0.69	0.97
3	Δ Torsional RF = 1.34 Δ UPV + 0.95	0.97

The linear relationships between these parameters indicate that the impact of micro-cracking on both RF and UPV reduction occurs at a consistent ratio. The dimensional representations of frequency and pulse

velocity are $[T^{-1}]$ and $[L.T^{-1}]$, respectively. These dimensions are influenced by the porosity of the specimens, which comprises both pores and micro-cracks. Notably, the pores remain constant in this context, distinguishing them from the micro-cracks. As a component in speed's dimension, the arrival time of the wave rises due to the changes that the appearance of microcracks makes on the length of the trajectory between the transmitters. Accordingly, the apparent speed decreases (Shen et al., 2020).

5. Conclusions

This study demonstrates that Blue Bateig limestone exposed to high temperatures shows significant thermal damage. Both ultrasonic pulse velocity and resonant frequency tests effectively captured the degradation extent, showing progressive mechanical integrity declines with increasing temperature. Key findings include:

1. UPV and RF values decrease significantly beyond 200°C, reflecting the initiation of thermal microcracking. The damage becomes severe at 600°C, with reductions in UPV and RF exceeding 30% and 40%, respectively.
2. The UPV and RF results show strong linear relationships in all RF types and every heat exposure target temperature.

The findings have practical implications in structures using Blue Bateig limestone, especially in fire-prone environments that need regular assessments of thermal damage. Since the methods used in this study are non-destructive and the equipment is relatively portable, these examinations can be conducted on-site. The practical applications of this technique in situ are within the scope of the authors' future research. Furthermore, the study enhances understanding of thermal behavior in carbonate rocks.

Acknowledgement

The authors acknowledge the Dept. of Geotechnical and Geological Engineering of Universitat Politècnica de València, Dept. of Civil Engineering of Universidad de Alicante, and Dept. Explotación y Prospección de Minas of Universidad de Oviedo, for its continuous support. This investigation was funded by the Conselleria de Innovación, Universidades, Ciencia y Sociedad Digital of Generalitat Valenciana through the program GE2024 - CIGE/2023/201. In addition, this research was funded by the Ministry of Science and Innovation of Spain through Grant MCINN-23-PID2022-142015OB-I00 funded by MCIN/AEI/10.13039/501100011033 and by 'ERDF A way of making Europe'.

References

- Altuğ, M., Soeylemeç, M. and Günaydın, O. (2023) Experimental Investigation of the Effect of High Temperature on the Mechanical Properties of Rocks Used as Building Blocks. *Iranian Journal of Science*, 47(1), pp.91-98.
- ASTM, C. (2008) Standard test method for fundamental transverse, longitudinal, and torsional resonant frequencies of concrete specimens. *Annual book of ASTM standards*, 69, p.50.
- Aydin, A. (2014) Upgraded ISRM suggested method for determining sound velocity by ultrasonic pulse transmission technique. In *The ISRM Suggested Methods for Rock Characterization, Testing and Monitoring: 2007-2014* (pp. 95-99). Cham: Springer International Publishing.
- Eljufout, T., & Alhomaïdat, F. (2021) Evaluation of natural building stones' characterizations using ultrasonic testing technique. *King Fahd University of Petroleum & Minerals*.
- Feng, Y., Su, H., Yin, Q., Yu, L. and Wang, Y. (2021) Experimental study on mechanical property and pore distribution of limestone specimens after heat treatment under different heating conditions. *Advances in Materials Science and Engineering*, 2021(1), p.9957330.
- Garrido, M.E., Martínez-Ibáñez, V., Signes, C.H., Serón Gáñez, J.B., Tomás, R. and Álvarez-Fernández, M.I. (2023) Point Load Strength Index of a Limestone Exposed to High Temperatures and Correlation with Uniaxial Compressive Strength. In *ISRM Congress* (pp. ISRM-15CONGRESS). ISRM.
- González-Gómez, W.S., Quintana, P., May-Pat, A., Avilés, F., May-Crespo, J. and Alvarado-Gil, J.J. (2015) Thermal effects on the physical properties of limestones from the Yucatan Peninsula. *International Journal of Rock Mechanics and Mining Sciences*, 75, pp.182-189.
- Hassanpour, J., Kazemi, C. and Rostami, J. (2024) Introduction of a modified QTBM model for predicting TBM penetration rate in rock, based on data from mechanized tunneling projects in Iran. *Bulletin of Engineering Geology and the Environment*, 83(5), pp.1-17.
- Kazemi, C. and Cheshomi, A. (2022) Crack Extension Analysis in Carbonate Specimens Under Brazilian Test Using DIC Method. *8th Iranian Rock Mechanics Conference*, Shahrood, Iran.
- Liu, D., Chen, H. and Su, R.K.L. (2024) Effects of heat-treatment on physical and mechanical properties of limestone. *Construction and Building Materials*, 411, p.134183.
- Martínez-Ibáñez, V., Benavente, D., Hidalgo Signes, C., Tomás, R. and Garrido, M.E. (2021a) Temperature-induced explosive behaviour and thermo-chemical damage on pyrite-bearing limestones: causes and mechanisms. *Rock Mechanics and Rock Engineering*, 54(1), pp.219-234.
- Martínez-Ibáñez, V., Garrido, M. E., Signes, C. H., & Tomás, R. (2021b) Micro and macro-structural effects of high temperatures in Prada limestone: Key factors for future fire-intervention protocols in Tres Ponts Tunnel (Spain). *Construction and Building Materials*, 286, 122960.
- Shen, H., Li, X., Li, Q. and Wang, H. (2020) A method to model the effect of pre-existing cracks on P-wave velocity in rocks. *Journal of Rock Mechanics and Geotechnical Engineering*, 12(3), pp.493-506.
- Shen, Y., Yang, Y., Yang, G., Hou, X., Ye, W., You, Z. and Xi, J. (2018) Damage characteristics and thermo-physical properties changes of limestone and sandstone during thermal treatment from -30 C to 1000 C. *Heat and Mass Transfer*, 54, pp.3389-3407.
- Tufail, M., Shahzada, K., Gençturk, B. and Wei, J. (2017) Effect of elevated temperature on mechanical properties of limestone, quartzite and granite concrete. *International Journal of Concrete Structures and Materials*, 11, pp.17-28.
- Yang, J., Fu, L.Y., Zhang, W. and Wang, Z. (2019) Mechanical property and thermal damage factor of limestone at high temperature. *International Journal of Rock Mechanics and Mining Sciences*, 117, pp.11-19.